Journal of Materials Science: Materials in Electronics (2020) 31:9076–9090
https://doi.org/10.1007/s10854-020-03540-2

REVIEW

Corrosion behavior of Sn-based lead-free solder alloys: a review

Shuai Li[1] · Xingxing Wang[1] · Zhongying Liu[1] · Yongtao Jiu[2] · Shuye Zhang[3] · Jinfeng Geng[4] · Xiaoming Chen[5] · Shengjin Wu[1] · Peng He[3] · Weimin Long[2]

Received: 3 March 2020 / Accepted: 2 May 2020 / Published online: 13 May 2020

Abstract
Sn-based lead-free solder alloys have been investigated widely to replace the traditional Sn–Pb solder alloys. Since the miniaturization of electronic products and the expansion of application field, the corrosion resistance of solder alloys play a key factor in the reliability of electronic products in long-term service. In this article, we review the recent progress on the corrosion behavior of Sn-based lead-free solder alloys by summarizing the results in representative ones of Sn–Bi, Sn–Cu, Sn–Zn, Sn–Ag, Sn–Ag–Cu and other multi-elements lead-free solder alloys. Specifically, the relationship between microstructure morphology and corrosion behavior, the corrosion mechanism of Sn-based lead-free solder alloys after incorporation of alloy elements or particles are summarized. It is hoped that this overview will provide some useful information in clarifying the corrosion mechanism and development of lead-free solder alloys. Furthermore, remaining difficulties and future trends in this research field are proposed.

1 Introduction

The electrical components are joined with solder alloys to achieve mechanical integration and electric connection in industry [1–4]. As we know, the Sn–Pb solder alloys are used widely in electronic field due to the optimal combination of satisfactory corrosion resistance, low cost and good wettability and mechanical properties etc. [5–7]. However, the Pb belongs to heavy metal toxin, which is harmful to the health and environment [8–11]. The worldwide researchers have paid much attention to the investigations of lead-free solder alloys. And then Sn-based lead-free solder alloys are considered as the most promising candidates of replacing the traditional Sn-Pb solder alloy in recent years. Several major Sn-based binary solders alloys were reported in the relevant investigations, such as Sn–Zn [12, 13], Sn–Cu [14–16], Sn–Ag [17] and Sn–Bi [3, 18–20] etc. To enhance the combination properties of lead-free solder alloys further, the ternary or multi-elements solder alloys are designed by alloy element additions and the Sn–Ag–Cu ternary lead-free solder alloys have been considered as the best choice of substituting the conventional Sn–Pb solder alloys [21–23]. The main difficulty in the development of lead-free solder alloys is to obtain the optimal combination of wettability, mechanical performance, electrical characteristic, corrosion resistance, cost etc [9].

Since the growing miniaturization of electric products and the deterioration of service environment, the corrosion problem of solder alloys becomes a critical factor in long-term service, especially in high-temperature and high-humidity conditions [24–28]. Although the corrosion occurred in electronic devices are the same as those observed in steel structure bridges, automobiles, pipelines and other familiar objects in daily life, however, the structural members electronic devices are very small with the evolution of integrated packaging technology. Therefore, the corrosion products with the nanogram or less can result in complete device failure [29]. The corrosion resistance

✉ Xingxing Wang
paperwxx@126.com

1 School of Mechanical Engineering, North China University of Water Resources and Electric Power, Zhengzhou 450045, China

2 State Key Laboratory of Advanced Brazing Filler Metals & Technology, Zhengzhou Research Institute of Mechanical Engineering, Zhengzhou 450001, China

3 State Key Laboratory of Advanced Welding and Joining, Harbin Institute of Technology, Harbin 150001, China

4 Electric Power Research Institute, State Grid Henan Electric Power Company, Zhengzhou 450052, China

5 Key Laboratory of Surface Engineering of Equipment for Hydraulic Engineering of Zhejiang Province, Standard & Quality Control Research Institute, Ministry of Water Resources, Hangzhou 310012, China

should be emphasized in the progress of new type solder alloys. As we know, the corrosion of solder joints involves interaction with the service environment. Consequently, the investigations on the corrosion resistance of lead-free solder alloys mainly focuses on the evolution of microstructure and the simulation of service environment at present. The research on microstructure of solder alloys focuses on the addition of metals or particles (alloy elements, rare earth and nanoparticles etc.) and the change in external factors (change of cooling rate and application of permanent magnet stirring). To simulate the service environment, the evolution of corrosion properties of solder alloys in the neutral, alkaline and acidic solutions were analyzed [8].

At present, the researches on the corrosion performance of Sn-based lead-free solder alloys are isolated and the relevant results are scattered, even some conclusions are contradictory. Consequently, a critical review on the corrosion properties of Sn-based lead-free solder alloys is necessary. In the present paper, the authors try to collect all the relevant data and information on the corrosion performance of Sn-based lead-free solder alloys from recent investigations and then provide some guidance in the future work. At present, the investigations mainly focused on the Sn–Zn, Sn–Cu, Sn–Ag, Sn–Bi, Sn–Ag–Cu and other multi-elements Sn-based lead-free solder alloys.

2 The fundamentals on the corrosion of lead-free solder alloys

The evolution of corrosion properties of Sn-based solder alloys is mainly associated with the transformation of microstructure. For Sn–Zn lead-free solder alloys, the galvanic corrosion formed between the Zn-rich phase and Sn-rich phase [30, 31]. And the corrosion of Sn–Bi solder alloys is attributed to the potential difference between the Zn-rich phase and Bi-rich phase. While for the Sn–Cu, Sn–Ag and Sn–Ag–Cu solder alloys, the galvanic corrosion formed between the Zn-rich phase and intermetallic compounds, and the intermetallic compounds mainly consist of Ag_3Sn and Cu_6Sn_5, which are nearly insoluble in corrosion medium due to the chemical stability [26, 32]. The corrosion performance of Sn-based leas-free solder alloys is analyzed by means of different experimental methods [33–36].

2.1 Formation of corrosion products

The formation of corrosion products of Sn-based lead-free solder alloys mainly involves in the dissolution of Sn-rich phase and Zn-rich phase. The corrosion products of ZnO, $Zn(OH)_2$ and $Zn_5(OH)_8Cl_2{\cdot}H_2O$ formed in Sn–Zn solder alloys. The corrosion produce starts with the dissolution of Zn at anodic sites in the NaCl solution [37–40]:

$$Zn \rightarrow Zn^{2+} + 2e^- \quad (1)$$

Then the cathodic reaction:

$$2H_2O + O_2 + 4e^- \rightarrow 4OH^- \quad (2)$$

The formation of ZnO and $Zn(OH)_2$ [37–40]:

$$Zn + 2OH^- \rightarrow Zn(OH)_2 + 2e^- \quad (3)$$

$$Zn(OH)_2 \rightarrow ZnO + H_2O \quad (4)$$

With the concentration of Cl^-, the corrosion product of $Zn_5(OH)_8Cl_2{\cdot}H_2O$ formed, the formation process as follows [37–40]:

$$ZnO + Zn^{2+} + 5H_2O + 2Cl^- \rightarrow Zn_5(OH)_8Cl_2 \times H_2O \quad (5)$$

For Sn–Cu, Sn–Ag, Sn–Bi and Sn–Ag–Cu solder alloys, the relevant investigations have proven that the corrosion products mainly consist of SnO, SnO_2, $Sn(OH)_4$ and $Sn_3O(OH)_2Cl_2$. The corrosion process starts with the dissolution of Sn at anodic sites [32, 35, 41–46]:

$$Sn \rightarrow Sn^{2+} + 2e^- \quad (6)$$

$$Sn^{2+} \rightarrow Sn^{4+} + 2e^- \quad (7)$$

And the cathodic reaction occurs according to the reaction (2). Then the SnO, SnO_2, $Sn(OH)_4$ formed, the details as follow [11, 32, 41–43, 45]:

$$Sn + 2OH^- \rightarrow Sn(OH)_2 + 2e^- \quad (8)$$

$$Sn(OH)_2 \rightarrow SnO + H_2O \quad (9)$$

$$SnO + H_2O + 2OH^- \rightarrow Sn(OH)_4 + 2e^- \quad (10)$$

$$Sn(OH)_2 + H_2O \rightarrow Sn(OH)_4 + 2e^- \quad (11)$$

$$Sn(OH)_4 \rightarrow SnO_2 + H_2O \quad (12)$$

Then the corrosion product of $Sn_3O(OH)_2Cl_2$ formed because of the presence of Cl^-, as follows [32, 41–43, 47]:

$$3Sn + 4OH^- + Cl^- \rightarrow Sn_3O(OH)_2Cl_2 + H_2O + 6e^- \quad (13)$$

2.2 Research methods for corrosion resistance

The contaminants play a key factor in corrosion process of solder alloys, especially the Cl^-. As the result, significant investigation efforts have been paid to study the evolution of corrosion susceptibility of lead-free solder alloys in NaCl solution. The immersion corrosion tests are performed to

evaluate the corrosion susceptibility of solder alloys in NaCl solution. This method can be applied to assess the corrosion performance of solder alloy initially, while it is different with the actual service conditions. Then, the salt spray service environment and the high-humidity and high-temperature service condition are created to simulate the service environment further [26, 32, 48, 49]. However, the researchers pointed out that the corrosion occurred in service of electronic devices belongs to atmospheric corrosion, which the electrochemical reactions occur under the thin electrolyte layer [50, 51]. Consequently, the corrosion resistance of solder alloys is investigated under a thin electrolyte layer [35, 36]. The above-mentioned experimental methods can only observe the evolution of corrosion morphology of solder alloys, while the corrosion mechanism should be analyzed by electrochemical experiments. The open circuit potential, potentiodynamic polarization and electrochemical impedance spectroscopy (EIS) tests are always conducted in electrochemical experiments. Then, the corrosion mechanism is discussed according to the obtained electrochemical parameters in electrochemical experiments.

3 Corrosion behavior of Sn-based lead-free solder alloys

3.1 Sn–Zn

Sn–Zn solder alloy is considered as an attractive candidate to substitute the Sn–Pb solder alloy owing to good comprehensive properties. The eutectic composition is Sn–9Zn with the welting temperature of 198 °C, which is relatively close to the conventional eutectic Sn–Pb solder alloy [52–54]. However, Sn–Zn solder alloy has higher corrosion susceptibility in corrosive medium environment owing to the presence of Zn. Consequently, the researchers have paid much attention on the corrosion resistance of Sn–Zn solder alloy.

The corrosion resistance of five Sn-based solder alloys were evaluated in the 0.1M NaCl solution [55]. It was found that the Sn–9Zn solder alloy existed the highest corrosion susceptibility due to the presence of negative Zn in NaCl solution. Furthermore, the corrosion mechanism of Sn–Zn solder alloy was investigated systematically by Liu et al. [30, 56, 57]. They reported the evolution of corrosion morphology of Sn–Zn solder alloy with different Zn addition in 0.5 M NaCl solution, the images are displayed in Fig. 1 [30]. It was found that the corrosion susceptibility of solder alloy increased with the increase of Zn content, which is associated with the formation of coarsening Zn-rich precipitates[30]. The susceptibility to metastable pitting of Sn–Zn solder alloy is mainly associated with the passive film properties and evolution of microstructure, and the susceptibility to pitting increases with the increase of Zn content [56, 57]. Furthermore, the pitting formation of Sn–Zn solder alloy can be divided into three stages (in Fig. 2): In first stage, the Cl^- permeated the oxide film through the intergranular boundaries gradually after the Cl^- adsorbed onto the passive film for a period of time; in the second stage, some tiny crack extended from the surface of passive film towards the interface between the film and Sn–Zn lead-free solder alloy. Finally, localized breakdown occurred due to the increase of internal stress [56]. The similar phenomenon was observed in the corrosion process of Zn–30Sn solder alloy in neutral NaCl solution [37].

According to the understanding of corrosion mechanism of Sn–Zn solder alloy, it is speculated that the corrosion susceptibility can be obviously suppressed by the modification of microstructure with doping of alloy elements or particles, the effect of alloy elements metals or particles on the corrosion susceptibility of Sn-based lead-free solder alloy is summarized in Table 1. It was found that all the Sn–9Zn–0.1x (x = Ni, Cr, Cu and Ag) solder alloys with doping of these elements improved the corrosion resistance obviously [31]. The tendency to suppress corrosion increased in the order of Ag < Cu < Cr < Ni [31]. Furthermore, it was found that the incorporation of Ti [58] and Mn [38] had obvious influence on the improvement of corrosion resistance of Sn–Zn solder alloy and the corresponding corrosion mechanism of solder alloys with the addition of different alloying elements were analyzed from the evolution of microstructure and formation of passive film [31, 38, 58]. Wang et al. [39] also confirmed that the doping Ti could decrease the corrosion susceptibility of Sn–9Zn when the addition was lower than 0.1%, and the optimized Ti content was 0.05%. Furthermore, the effect of addition of Cr content (x = 0, 0.1, 0.3 and 0.5 wt%) on the corrosion susceptibility of Sn–8.5Zn solder alloy in 3.5 wt% NaCl solution was analyzed according to potentiodynamic polarization results [47]. They pointed out that the doping of Cr could result in the change of anodic polarization characterics. The best corrosion resistance of the Sn–8.5Zn solder alloy in the NaCl solution were obtained when the addition of Cr is 0.3 wt% [47].

Furthermore, the addition of Ag [52], In [59] and Ga [60] could decrease the corrosion susceptibility of Sn–9Zn solder alloy, while the Al doping had opposite effect.

The investigations mentioned above mainly focused on the corrosion susceptibility of Sn-based solder alloy in NaCl solution. The alkaline environment may exist in the service of electronic devices. The corrosion susceptibility of Sn–Zn solder alloy in 6 M KOH solution was investigated based on potentiodynamic polarization experiment results by Nazeri et al. [61]. It was found that the corrosion potential (E_{corr}) of Sn–Zn solder alloys had no obvious change when the Zn content changed from 0 to 12 wt%, while the corrosion current density(i_{corr}) increased

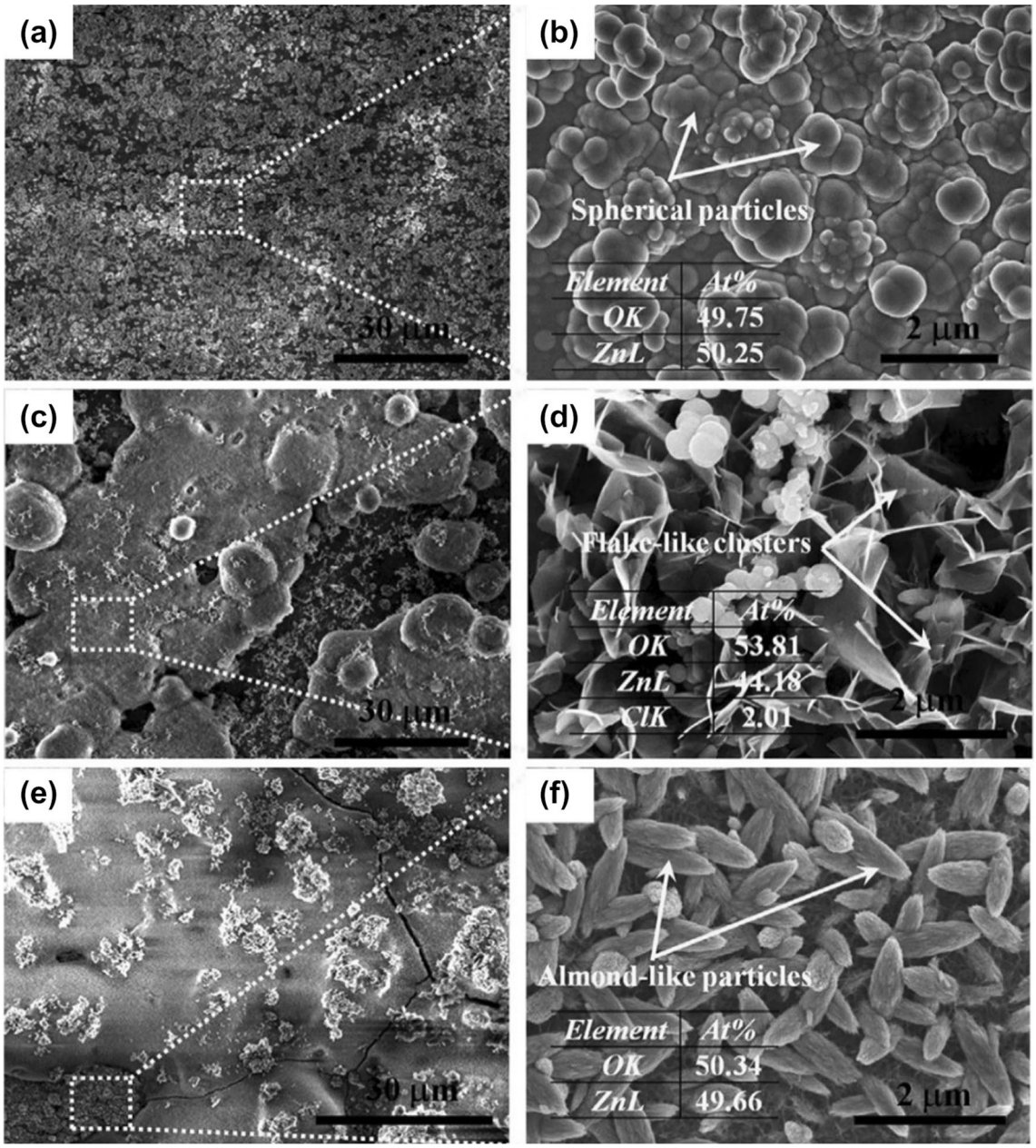

Fig. 1 The corrosion morphology of Sn–Zn alloys after immersion in 0.5 M NaCl solution for 7 days: **a** and **b** Sn–6.5Zn, **c** and **d** Sn–9Zn, **e** and **f** Sn–12Zn [30]

significantly. The co-existed corrosion products of ZnO, SnO_2 and SnO formed on the surface of Sn–Zn solder alloy after polarization experiment, which indicated the formation of passive film [61]. Additionally, it was found that the ultimate tensile stress of Cu/Sn–9Zn/Cu solder joint reduced by 26% after polarization in 6 M KOH solution due to the grooves caused by the dissolution of negative Zn [62]. The ultimate tensile stress of Cu/Sn–9Zn/Cu solder joint also decreased after open circuit potential (OCP) experiment [53].

3.2 Sn–Cu

Sn–Cu solder alloy is also one of the potential successor of replacing the Sn–Pb solder alloy due to the advantage of low cost and good comprehensive performance. The eutectic alloy with melting point of 227 °C formed when the addition of Cu is 0.7% [63]. The corrosion reason of Sn–Cu solder alloys is the formation of galvanic couples between the Sn-rich matrix and Cu–Sn intermetallic compounds, and the evolution of microstructure results in the change of corrosion susceptibility of solder alloys.

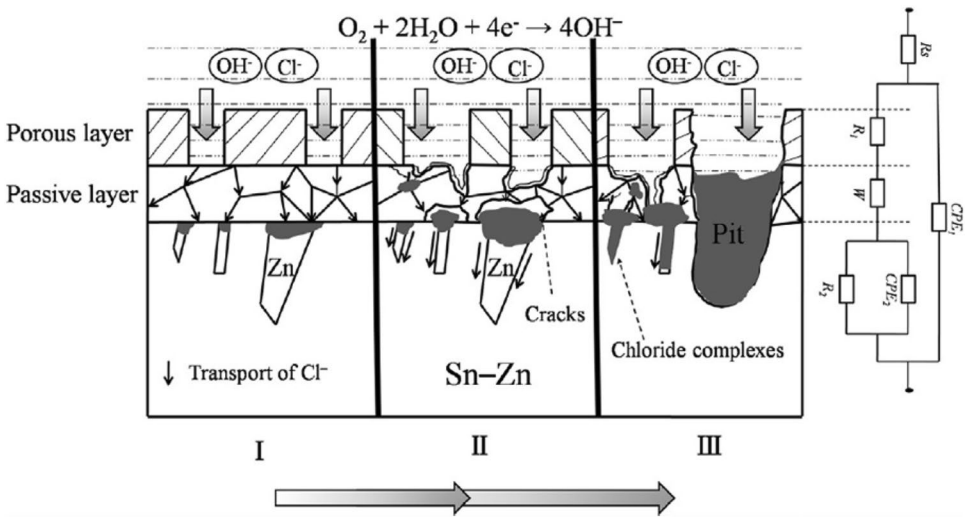

Fig. 2 Schematic diagram of pitting corrosion mechanism in NaCl solution [56]

The comparative analyses of the corrosion susceptibility of Sn–Pb solder alloy and other lead-free solder alloys (Sn–Cu, Sn–Ag and Sn–Ag–Cu) were performed [41]. They pointed out that the lead-free solder alloys existed lower corrosion susceptibility than that of Sn–Pb solder alloy in 3.5 wt% NaCl solution [41]. However, Sn–37Pb solder alloy exists the lowest corrosion susceptibility and Sn–3.0Ag–0.5Cu solder alloy has the lowest corrosion resistance among four solder alloys (Sn–37Pb, Sn–0.7Cu, Sn–3.0Ag and Sn–3.0Ag–0.5Cu solder alloys) under the condition of fire smoke produced from the burning of polyvinyl chloride [64]. Additionally, it was found that the corrosion susceptibility of four studied solder alloys increased with the increase of smoke concentrations.

The cooling rate of solidification play a key role on the evolution of corrosion properties of lead-free solder alloys [9, 65, 66]. Osório et al. [65, 66] studied the corrosion susceptibility of Sn–2.8Cu solder alloy in 0.5 M NaCl solution obtained with different solidification cooling rate. They found that fine and homogeneously distributed Cu–Sn intermetallic compounds formed in the Sn-rich matrix when the cooling rate is around 15 °C/s, and the coarsening microstructure appeared with the cooling rate of around 1.2 °C/s. Then the corresponding corrosion current density of the former is about two times higher than that of the latter [65]. The variation of corrosion resistance of Sn–2.8Cu solder alloys with different cooling rate is related to both localized strains between the Sn-rich phase and Cu–Sn intermetallic compounds and the cathode/anode area ratios [66]. The schematic diagram of correlation between the typical microstructure and the evolution of corrosion is shown in Fig. 3 [66]. Freitas et al. [67] also demonstrated that the cooling rate had apparent influence on the corrosion susceptibility and mechanical strength of Sn–0.7Cu solder alloy. It was found that the fine dendritic branches and fibrous Cu_6Sn_5 intermetallic compound are harmful to the corrosion properties of Sn–0.7Cu solder alloy, while it is beneficial for the mechanical strength.

The addition of alloy elements or particles into solder alloys is a valid way to modify the corrosion susceptibility of Sn–Cu solder alloy, the details is summarized in Table 1. Jaffery et al. [10] reported the influence of the addition of Fe and Bi on the corrosion susceptibility of Sn–0.7Cu solder alloy in 3.5 wt% NaCl solution. It was found that the corrosion resistance deteriorated after doping of Fe and Bi owing to the formation of $FeSn_2$ and Bi-rich phase [10]. While the incorporation of S could improve the corrosion properties of Sn–Sn–0.7Cu solder alloy due to the formation of passivating corrosion product of $Sn_3O(OH)_2Cl_2$ [42]. The evolution of the corrosion resistance of Sn–0.7Cu–0.075Al solder alloy by the addition of Ce and La on was studied by Yang et al. [68]. It was found that the addition of Ce and La enhanced the corrosion resistance of solder alloy [68]. Additionally, Huang et al. [69] investigated the influence of P on the corrosion susceptibility of Sn–0.7Cu solder alloy in the aggressive conditions. It was found that the doping of P could decrease the corrosion susceptibility of Sn–0.7Cu solder alloy. Furthermore, the corrosion rate of the solder alloy is lower in alkaline solution compared to that in acidic solution, while Yan et al. [70] point out that the addition of P had no evident influence on the corrosion susceptibility of Sn–0.7Cu solder alloy in simulated marine atmosphere. Moreover, Yan et al. [33, 70] studied the doping of Ga on the influence of the corrosion susceptibility of Sn–0.7Cu solder alloy in simulated marine atmosphere and demonstrated that the addition of Ga significantly reduced the corrosion susceptibility of solder alloy.

Table 1 Summary of the effect of alloy elements or particles incorporation on the corrosion susceptibility of Sn-based lead-free solder alloys

Solder alloys	Addition	Microstructure	Corrosion resistance	Corrosive medium
Sn–9Zn	Ti [39, 58]	Refine Zn-rich precipitates; Sn_3Ti_2 and Sn_5Ti_6	↑	0.5 M NaCl
Sn–9Zn	Mn [38]	Refine Zn-rich precipitates; Zn_6Sn_2Mn	↑	0.5 M NaCl
Sn–9Zn	Ga [60]	Refine Zn-rich precipitates	↑	3.5 wt% NaCl
Sn–Zn	Zn [30, 56, 57]	Coarse Zn-rich precipitates	↓	0.5 M NaCl
Sn–9Zn	Ni [31]	Refine Zn-rich precipitates; Ni_5Zn_{21}	↑	0.5 M NaCl
Sn–9Zn	Cr [31]	Refine Zn-rich precipitates; Sn_2Zn_6Cr	↑	0.5 M NaCl
Sn–9Zn	Cu [31]	Refine Zn-rich precipitates; Cu_5Zn_8	↑	0.5 M NaCl
Sn–9Zn	Ag [31, 52]	Refine Zn-rich precipitates; $AgZn_3$	↑	0.5 M NaCl
Sn–Zn	Al [60, 112]	Coarse Zn-rich precipitates	↓	3.5 wt% NaCl
Sn–9Zn	In [59]	Refine Zn-rich precipitates; In_3Sn	↑	6 M KOH
Sn–8.5Zn	Cr [47]	Refine Zn-rich precipitates; $Cr_2Sn_2(Zn)$	↑	3.5 wt% NaCl
Sn–9Zn	Ni [113]	Ni_3Sn_4	↑	5 wt% NaCl
Sn–0.7Cu	Fe and Bi [10]	$FeSn_2$ and Bi-rich phase	↓	3.5 wt% NaCl
Sn–0.7Cu	S [42]	SnS	↑	3.5 wt% NaCl
Sn–0.7Cu–0.075Al	Ce and La [68]	Refine grains; CeO_2 and La_2O_3	↑	3.5 wt% NaCl
Sn–0.7Cu	Al [69]	–	↑	NaOH
Sn–0.7Cu	Al [70]	–	-	Simulated seawater
Sn–0.7Cu	Ga [33, 70]	Ga_2O_3	↑	Simulated seawater
Sn–1.0Ag	Ce [82]	Refine grains and precipitates	↑	100 mM Na2SO4+ 3 mM chloride ion addition
Sn–3.5Ag	CeO_2 [83]	Refine Ag_3Sn	↑	3.5 wt% NaCl
Sn–Ag	Cu [84]	Coarse Ag_3Sn and Cu_6Sn_5	↑	0.1M NaCl
Sn–*x*Ag	Ag [74]	Volume fraction of the Ag_3Sn	↑	0.3 wt% Na_2SO4
Sn–*x*Ag	Ag [11]	Refine Ag_3Sn and Cu_6Sn_5	↑	3.5 wt% NaCl
Sn–1.0Ag–0.5Cu	Zn [45]	–	↓	3.5 wt% NaCl
Sn–3.0Ag–0.5Cu	Zn and In [96]	–	↓	3.5 wt% NaCl
Sn–3Ag–0.5Cu	Al [97]	–	↓	3.5 wt% NaCl
Sn–1Ag–0.5Cu	Ni [98]	–	↑	3.5 wt% NaCl
Sn–3.0Ag–0.5Cu	Graphene nanosheets [99]	Refine intermetallic compounds	↑	3.5 wt% NaCl
95.8Sn–3.5Ag–0.7Cu	Ni-coated carbon nanotubes [100]	–	↑	3.5 wt% NaCl
Sn–0.3Ag–0.7Cu	Al_2O_3 [101]	Refine intermetallic compounds	↑	0.5 M NaCl
Sn–8.5Zn–*x*Ag–0.1Al–0.5Ga	Ag [106, 107]	–	↑	3.5 wt% NaCl
Sn–8.5Zn–0.5Ag–*x*Al–0.5Ga	Al [108]	–	↑	3.5 wt% NaCl
Sn–8.5Zn–0.5Ag–Al–*x*0.5Ga	Ga [109]	–	↑	3.5 wt% NaCl
Sn–9Zn–3Bi–xCr	Cr [111]	–	↑	3.5 wt% NaCl
Sn–9Zn–0.5Ag–1In	In [110]	–	↑	3.5 wt% NaCl

1. ↑ Means the improvement of corrosion resistance; ↓ Stands for the reduction of corrosion resistance
2. All solder alloys ratios are a percentage of weight unless specially stated

3.3 Sn–Ag

Sn–Ag-based solder alloy have been considered to be a promising candidates to substitute the traditional Sn–Pb solder alloys owing to the better mechanical strength than that of the Sn–Pb solder alloys. The eutectic composition for the Sn–Ag binary system occurs at Sn–3.5Ag with the melting temperature of 221 °C [71–73]. The corrosion susceptibility of the Sn–Ag-based solder alloy is mainly associated with the galvanic corrosion between the Sn-rich phase and Ag_3Sn intermetallic compound [8, 74–76]. It had been reported that the scale, size and distribution of Sn-rich precipitates in matrix and Ag_3Sn particles of solder alloy played a key factor on the effect of corrosion resistance, mechanical and thermal properties [43, 77–81].

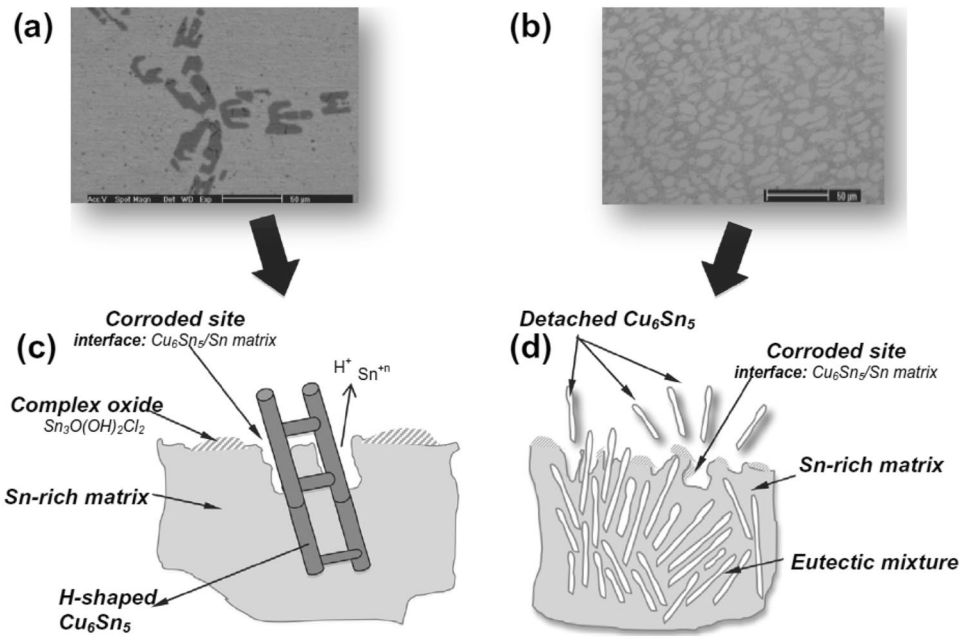

Fig. 3 Images of representative microstructures of Sn–Cu alloys: **a** Sn–2.8 Cu; **b** Sn–0.7 Cu alloys; **c** H-shaped Cu_6Sn_5 and Sn-rich phase and **d** eutectic mixture [66]

The corrosion susceptibility of Sn–0.3Ag–0.9Zn solder alloy with different cooling methods was evaluated in 3.5 wt% NaCl solution according to the electrochemical experimental results[43]. It was found that the corrosion susceptibility of water-cooled solder alloy was lower than those of furnace-cooled and air-cooled solder alloys, which was associated with the types, size and distribution of precipitates. It also demonstrated that the barrier property of passive film formed with different cooling methods was various. Moreover, Osório et al. [81] confirmed that the corrosion susceptibility of Sn–2Ag solder alloy with higher cooling rate is lower than that of solder alloy with lower cooling rate. They pointed out the evolution of corrosion resistance was associated with evolution of morphology of Ag_3Sn.

The microstructure of solder alloy can be modified by the alloy addition of alloy elements or particles, then results in the change of corrosion resistance and mechanical properties. Vuong et al. [82] demonstrated that the incorporation of Ce in Sn–1.0Ag solder alloy improved the corrosion resistance in the naturally-aerated 100 mM Na_2SO4 with 3 mM chloride ion addition solution, which is attribute to the Ce acceleration of the passive film formation. Moreover, it was found that the doping of CeO_2 nanoparticles could affect the corrosion susceptibility of Sn–3.5Ag solder alloy in 3.5 wt% NaCl solution and the best doping of CeO_2 nanoparticles was about 12% judging from the corrosion resistance [83].

The corrosion resistance of traditional Sn73.9Pb26.1 solder and the Sn–Ag–M (M = In, Bi, Cu) solder alloys in 0.1 M NaCl solution was investigated by Rosalbino et al. [84]. It was found that the Sn–2.3Ag–9.0In and Sn–3.0Ag–10.4Bi solder alloys had higher corrosion susceptibility compared to traditional Sn–26.1Pb. However, the corrosion resistance of Sn–Ag solder alloy improved obviously with the Cu addition, which is higher than that of Sn–26.1Pb solder alloy. Bui et al. [74] studied the evolution of corrosion resistance of Sn–Ag solder alloy with different Ag content in Na_2SO_4 solution and found that the corrosion susceptibility of solder alloy increased with the increase of Ag content. It was found that the volume fraction of Ag_3Sn intermetallic compound rose with the increase of Ag content, then resulted in the increase of microgalvanic cell. However, Tunthawiroon et al. [11] demonstrated that the Ag content had little influence on the corrosion susceptibility of Sn–Ag solder alloy.

3.4 Sn–Bi

The Sn–Bi solder alloy is also regarded as a potential successor for traditional Sn–Pb solder alloys. Sn–58Bi is the eutectic composition for the Sn–Bi system, and the melting point is 138 °C [8, 85–87]. A few researches have been performed on corrosion of Sn–Bi solder alloys.

Satizabal et al. [8, 87] compared the corrosion resistance of Sn–10Bi solder alloy with Sn–2Ag and Sn–22Pb solder alloys in 0.15 M NaCl solution. They pointed out that the change of corrosion susceptibility is related to the solute contents, which determined the microstructural change, eutectic fraction and cathode to anode area ratios. The corrosion susceptibility ranks of three solder alloys in the following order: Sn–22Pb > Sn–2Ag > Sn–10Bi. Mostofizadeh et al. [88] revealed that the corrosion deteriorated the mechanical properties of Sn–Bi solder alloy. Additionally, Li et al. [81] investigated the doping of the nanoscale Cu_6Sn_5 particles on the influence of corrosion susceptibility of Sn–Bi solder alloys, and demonstrated that the corrosion

rate of Sn58Bi solder alloy with nanoparticles is suppressed obviously.

3.5 Sn–Ag–Cu

The ternary Sn–Ag–Cu solder alloys has been applied in electronic packaging. At present, the worldwide recommended chemical composition of Sn–Ag–Cu solder alloys are different. The Sn–3.9Ag–0.6Cu solder alloy is recommended in reflow soldering by the USA National Electronic Manufacturing Association [89] and the Sn–3.8Ag–0.7Cu solder alloy is suggested by Europe [90, 91]. While the Japan tends to recommend Sn–3.0Ag–0.5Cu (SAC305) solder alloy as the candidate of Sn–Pb solder alloy [1, 92, 93].

The Sn–Ag–Cu solder alloy has lower corrosion susceptibility compared to traditional Sn–Pb solder in 0.1 M NaCl solution, which is associated with the formation of a more compact passive film on the surface of Sn–Ag–Cu solder alloy [94]. Furthermore, they also indicated that the SAC305 solder existed lower corrosion susceptibility compared to SAC305 solder [95].The investigations of incorporation of alloy elements or particles into solder alloys were also performed to improve the corrosion resistance. Subri et al. [44] evaluated the influence of additions of Fe and Bi on the corrosion resistance of SAC105 solder alloy by means of potentiodynamic polarization experiment, and pointed out that the incorporation of 1 wt% Bi and 0.05 wt% Fe deteriorated the corrosion resistance of SAC105 in neutral solution and the immersion corrosion experiments indicated that the corrosion mass loss decreased in the order: Sn–1Ag–0.5Cu–Fe–1Bi < Sn–1Ag–0.5Cu < Sn–1Ag–0.5Cu–Fe–2Bi. The evolution of corrosion resistance was related to the change of microstructure, which induced the transformation of galvanic corrosion between the Ag_3Sn intermetallic compound and the Sn-rich phase. Furthermore, Liyana et al. [45] demonstrated that corrosion susceptibility increased with the increase of Zn addition content in 3.5 wt% NaCl solution. Hua et al. [96] also confirmed that the addition of Zn deteriorated corrosion resistance of SAC305 solder in 3.5 wt% NaCl salt solution. Additionally, it was found that the In addition was harmful to the corrosion properties of solder alloy [96]. At present, there is no agreement about the effect of the addition Al on the corrosion properties of Sn–Ag–Cu solder alloy. Fayeka et al. [46] pointed out that the corrosion susceptibility of SAC305–xAl(x =0, 0.1, 0.5) solder alloy increased with the doping of Al in 3.5 wt% NaCl solution according to electrochemical experiment results. However, Nordin et al. [97] revealed that the addition of Al decreased the corrosion susceptibility of SAC105–xAl solder (x = 0.2 wt%, 0.5 wt% and 1.0 wt%) in 5% NaCl solution judging from the potentiodynamic polarization and salt spray exposure experiments. Moreover, the doping of Ni on the effect of corrosion susceptibility of SAC105 in 3.5% NaCl solution was studied [98]. They pointed out that the Sn–1Ag–0.5Cu–0.05Ni and Sn–1Ag–0.5Cu–1Ni solder alloys showed better corrosion resistance compared to Sn–1Ag–0.5Cu–0.5Ni solder alloy [98].

The nanoparticles are also added to modify the corrosion susceptibility of the Sn–Ag–Cu solder alloys. It had demonstrated that the corrosion resistance of SAC305 solder alloy increased with incorporation of graphene nanosheets (GNSs) and the optimal addition is 0.03 wt% by Xu et al. [99]. Han et al. [100] conformed that the doping of Ni-coated carbon nanotubes (Ni-CNTs) suppressed the initiation and propagation of corrosion of SAC307 solder alloy in 3.5 wt% NaCl solution. Additionally, the addition of Al_2O_3 nanoparticles could enhance the corrosion resistance of SAC307 solder alloy in 0.5 M NaCl solution [101].

In order to obtain accurate assessment of corrosion behavior in actual conditions. The evolution of corrosion resistance of Sn–Ag–Cu solder alloy was investigated under high-temperature and high-humidity condition. Wang et al. [26, 32, 49] investigated the corrosion properties of SAC305 solder alloy systematically under high-temperature and high-humidity condition. It was found that the corrosion behavior of air-cooled and furnace-cooled SAC305 solder alloy was similar under the condition of 75 °C and relative humidity of 100%, which was worse than that of commercial SAC305 solder alloy. The deterioration of corrosion resistance of air-cooled and furnace-cooled solder alloy was associated with the coarsening of Ag_3Sn intermetallic compound, which caused by the change of cooling rate [26, 32, 49]. The thickness of the passive film increased with the increase of testing temperature (45, 65 and 75 °C) [26, 48, 49]. Moreover, the passive behavior of solder alloy was different in 3.5% NaCl solution at different temperatures (25, 45 and 65 °C) [32]. They also revealed that the corrosion susceptibility of solder joint increased because of the galvanic corrosion between the Sn-rich phase and Cu pad, which worse the reliability of solder joint [92].

It was found that crystallographic texture and aging treatment had obvious influence on the corrosion properties of lead-free solder alloys [7, 102, 103]. Daly et al. [95] studied the corrosion susceptibility of SAC205 solder alloy solidified with magnet stirring. They found that the corrosion susceptibility of SAC205 solder alloy decreased with permanent magnet stirring and the change in corrosion susceptibility of solder was relate to the transformation of microstructure (in Fig. 4) and crystallographic texture. Moreover, they also demonstrated that the corrosion always propagated along prismatic [103] planes easily in such crystals. Liu et al. [7] and Lee et al. [104] studied the long-term reliability of wafer-level packages SAC305 solder interconnects after 5% NaCl salt spray pretreatment. The images of a single SAC305 solder ball is shown in Fig. 5 [7]. Local corrosion

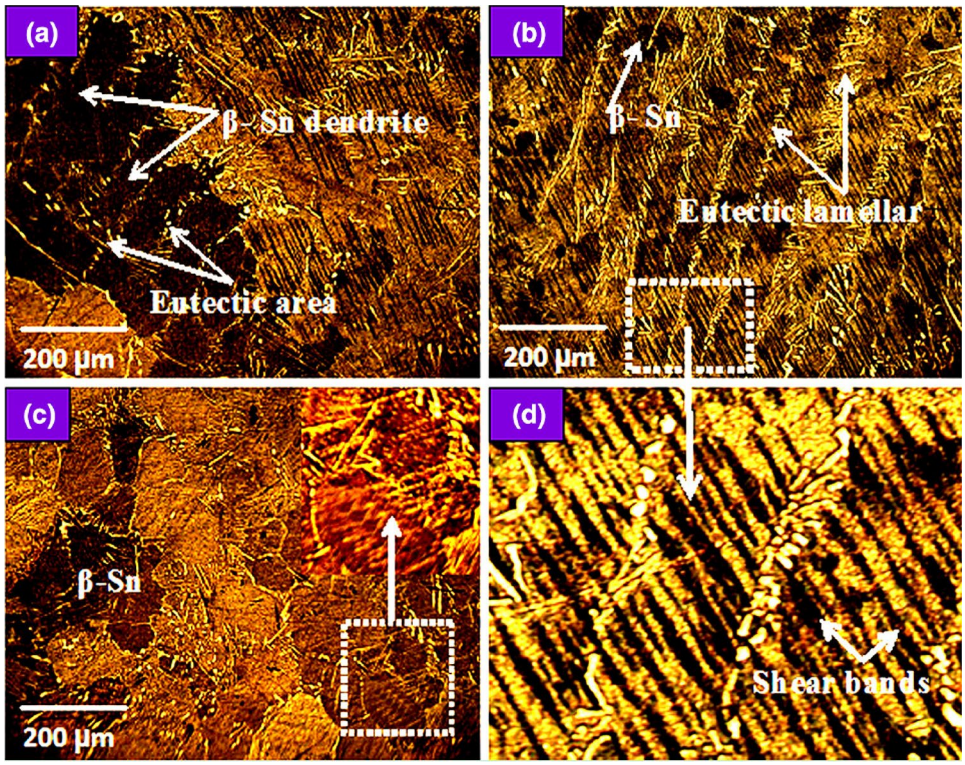

Fig. 4 The microstructures of as-solidified SAC205 solder alloy specimens **a** and **b** without permanent magnet stirring (PMS) **c** with PMS and **d** the magnified images of inset in **b** showing the shear bands in SAC205 solder alloy specimen without applying PMS [102]

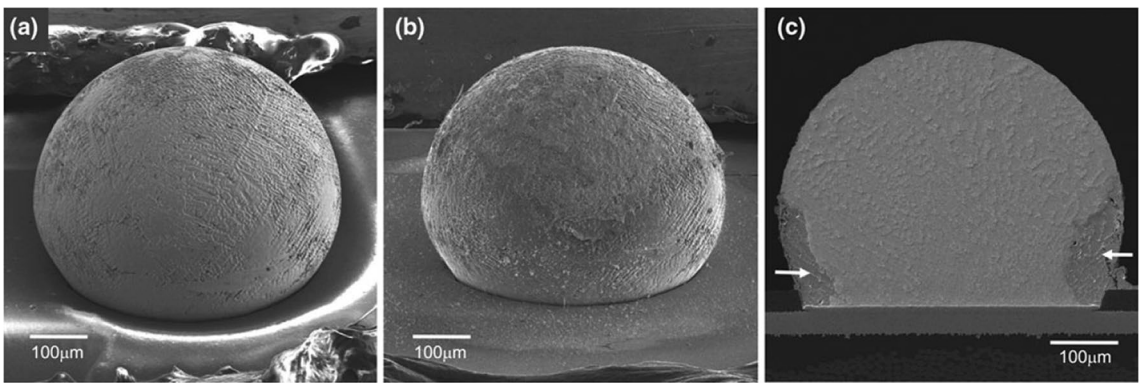

Fig. 5 SEM picture of a single SAC305 solder joint: **a** without 5% NaCl salt spray treatment and **b** after salt spray treatment for 96 h, and **c** cross-section morphology of SAC305 solder joint after conducted in 5% NaCl solution for 96 h [7]

occurred near the corner of the solder joint. The thermal cycle aging were carried out after 5% NaCl pretreatment to evaluated the long-term reliability, and the images are displaed in Fig. 6 [7]. They pointed out that obvious corrosion phenomenon appeared at the package-side interface corners of SAC305 solder joint and the corrosion propagation path displayed a distinguishable direction, as shown in Fig. 6b–d [7]. The orientation image microscopy (OIM) results demonstrated that the direction of corrosion propagation path was attributed to the Sn grain orientation, the details as shown in Fig. 7 [103]. Wang et al. [104] also revealed that reliability of SAC305 solder alloy were affected obviously by corrosion by means of in-situ three-point bending experiment and the fracture always initiated in the corroded locations. Moreover, Kaushik et al. [105] demonstrated that the aging treatment had beneficial influence on the improvement of corrosion resistance of Sn–Ag–Cu solder alloy, and the evolution reason is mainly related to the change of distribution, size and morphology of Cu_6Sn_5 and Ag_3Sn intermetallic compounds.

The corrosion of solder alloy in electronic components always suffered to atmospheric corrosion, which caused by a thin liquid film attached to the surface of solder alloy under high-temperature and high-humidity conditions. The corrosion behavior of solder alloys in thin electrolyte

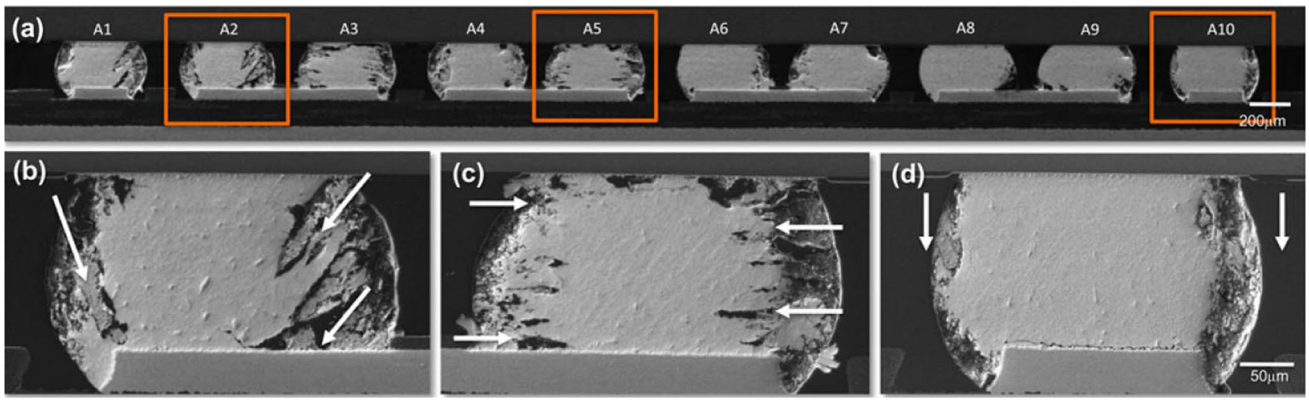

Fig. 6 The corrosion morphology of 5% NaCl preconditioned specimen after thermal cycles: **a** the samples of A1 to A10. Higher-magnification morphology of **b** joint A2, **c** joint A5, and **d** joint A10 [7]

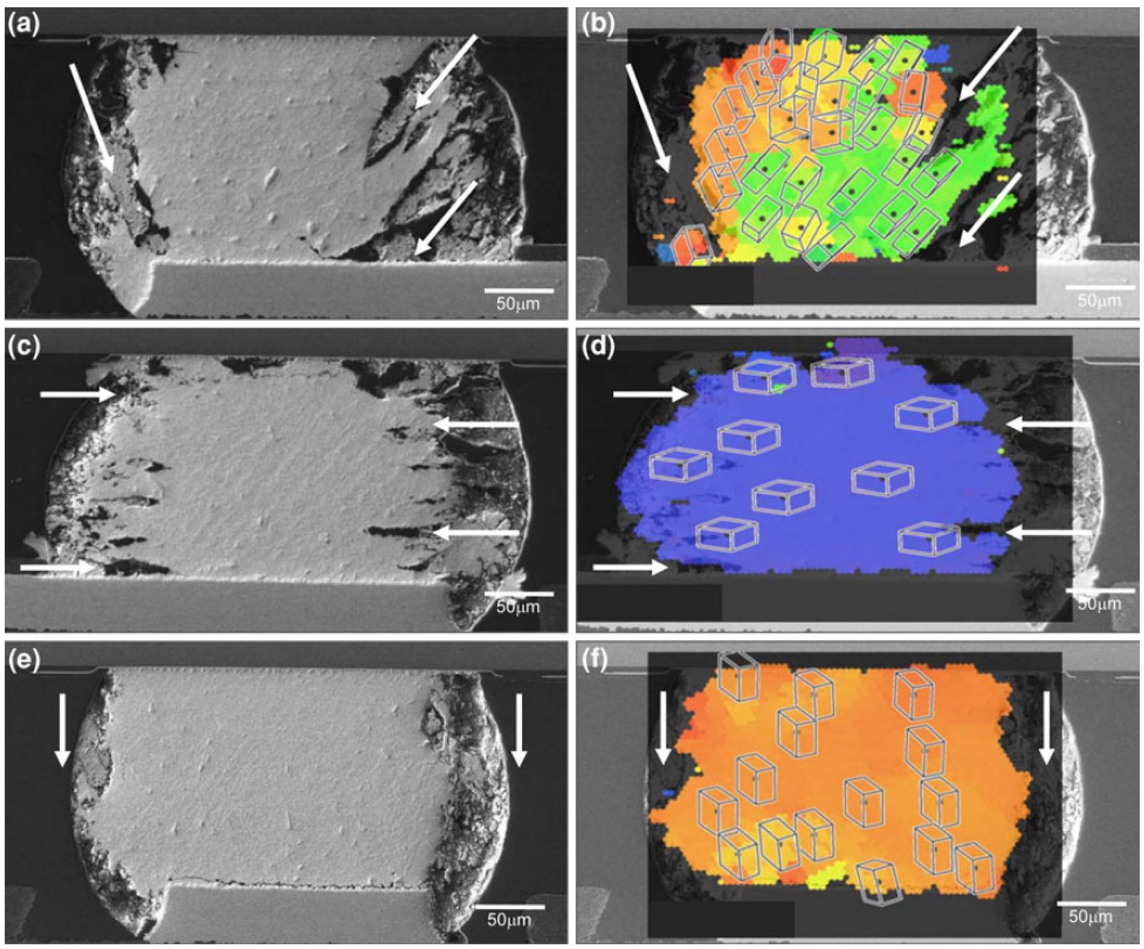

Fig. 7 Higher-magnification pictures and OIM maps for 5% NaCl preconditioned joints A2 (**a**, **b**), A5 (**c**, **d**), and A10 (**e**, **f**), display the correlation between the corrosion attack and the Sn lattice basal planes [103]

layer were different obviously compared to solution environment [35, 36]. Liao et al. [35] constructed the electrolyte layer thickness measurement and electrochemical experiment devices, as illustrated in Fig. 8. A thin electrolyte layer formed between the observation devices and experimental samples after the corresponding device

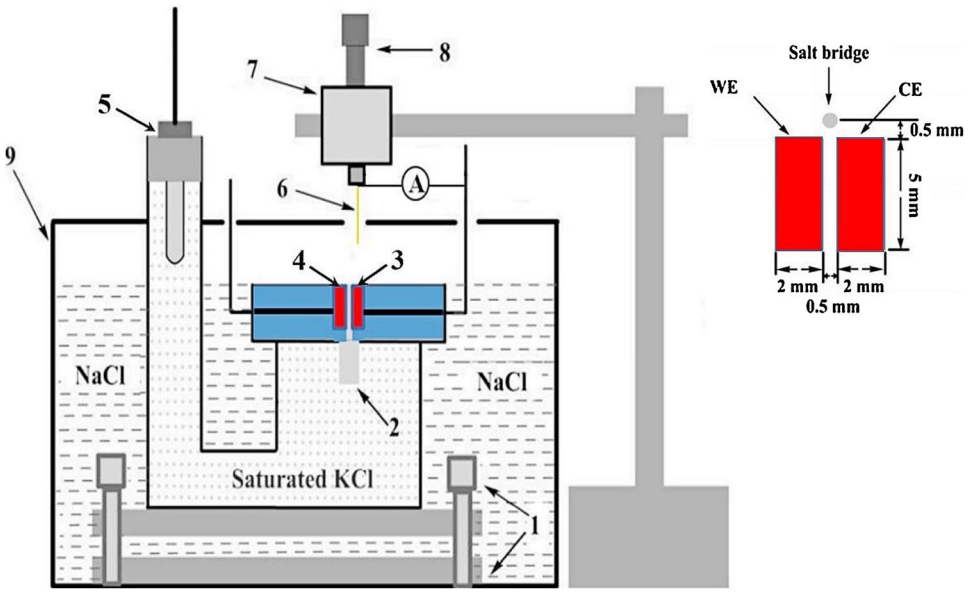

Fig. 8 Schematic diagram of experimental device for measurement of electrolyte layer thickness and electrochemical experiment setup: (1) Longitudinal stage, (2) KCl agar, (3) Working electrode, (4) Auxiliary electrode, (5) Reference electrode, (6) Platinum wire, (7) Mobile setup, (8) Micrometer, (9) Teflon box [35]

parts were fixed. They studied the corrosion resistance of SAC305 solder alloy in thin electrolyte layer under the conditions of 25 °C temperature of and 65% relative humidity. They pointed out that the solder alloy mainly presented pitting corrosion in chlorine-containing thin electrolyte layers, and the evolution of pitting corrosion can be divided into three stages, namely formation stage, accelerated growth stage and stable growth stage of pitting corrosion, as shown in Fig. 9.

3.6 Other multi-elements solder alloys

The other multi-component solder alloys are prepared on the basis of Sn–Zn binary solder alloys. Mohanty et al. [106–109] designed the five-elements solders based on the Sn–8.5Zn binary solder alloy by the additions of Ag [106, 107], Al [108], Ga [109]. Then the influence of the doping content of Ag, Al and Ga on the corrosion resistance of solder alloy in 3.5% NaCl solution was studied based on electrochemical experiments, respectively. It was found that the corrosion current density decreased and the corrosion potential shifted to noble direction of solder alloys when the Ag content increased from 0.1 to 1.5

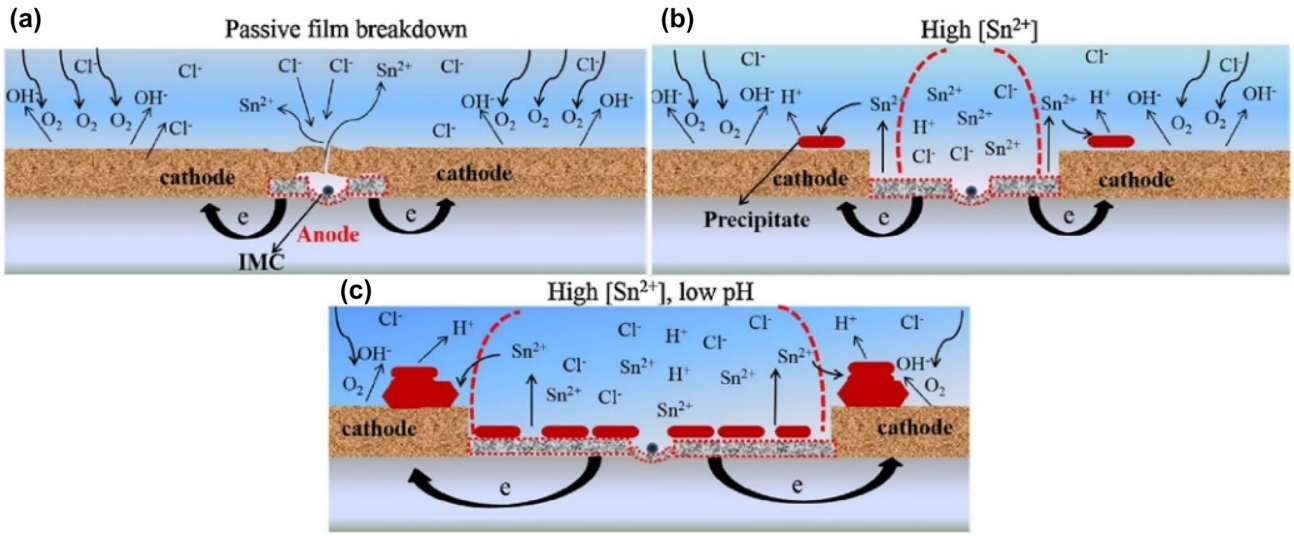

Fig. 9 Model of the evolution mechanism of pitting corrosion for SAC305 solder alloy under a thin electrolyte layer containing chlorine: **a** formation stage, **b** accelerated growth stage, **c** stable growth stage [35]

wt% [106]. The similar change tendency were also observed in the change of polarization resistance and corrosion rate of solder alloy [106]. The passivation of the Sn–Zn–*x*Ag–Al–Ga solders occurred when the Ag content is more than 0.1 wt% [106, 107]. And the corrosion susceptibility of the Sn–8.5 Zn–0.5 Ag–*x*Al-0.5 Ga solder alloys progressively increased with the increase of Al addition from 0.1 to 1.5 wt% [108]. They also confirmed that the doping of Ga had significantly influence on the corrosion resistance of Sn–8.5Zn–0.5Ag–0.1Al–*x*Ga [109]. Chang et al. [110] confirmed that the incorporation of In had no obvious effect on the corrosion performance of Sn–9Zn–0.5Ag solder alloy and it showed lower corrosion susceptibility than that of Sn–9Zn solder alloy. Additionally, Hu et al. [111] demonstrated that the doping of trace Cr could suppress the corrosion of Sn–9Zn–3Bi–*x*Cr solder according to the potentiodynamic polarization experiments in 3.5 wt% NaCl solution and the best addition is 0.5% considering the corrosion resistance.

4 Summary and conclusions

In summary, we proposed a concise review of the correlation between the microstructure and corrosion behavior, the evolution mechanism of corrosion resistance of solder alloys after the addition of alloy elements or particles. The results of these researches confirmed that the evolution of corrosion behavior of Sn-based lead-free solder alloys are mainly related to the transformation of microstructure and it is feasible to improve the corrosion resistance of solder alloys by addition of alloy elements or particles. However, the qualitative evaluation of the correlation between microstructure and corrosion resistance is of little significance to actual production. It is necessary to reveal the relationship between microstructure and corrosion behavior quantitatively based on multi-scale characterization. It is well-known that the solder alloys exist in the form of solder joint in practical condition and the package substrate increase the risk of galvanic corrosion. Nevertheless, most of existed investigations focused on the solder alloys. Furthermore, the investigations of evolution of corrosion behavior of Sn-based lead-free solder alloys during thermal aging should be emphasized.

Acknowledgments This research was funded by Research Foundation for High-level talent Scholars in North China University of Water Resources and Electric Power (No. 201811034) and Open Fund of National Joint Engineering Research Center for abrasion control and molding of metal materials (No. HKDNM2019020).

Reference

1. S. Li, Y.F. Yan, Intermetallic growth study at Sn-3.0Ag-0.5Cu/Cu solder joint interface during different thermal conditions. J. Mater. Sci. Mater. Electron. **26**, 9470–9477 (2015)
2. S. Zhang, B. Zhu, X. Zhou et al., Wettability and interfacial morphology of Sn-3.0Ag-0.5Cu solder on electroless nickel plated ZnS transparent ceramic. J. Mater. Sci. Mater. Electron. **30**, 17972–17985 (2019)
3. S. Zhang, T. Lin, P. He et al., Effects of acrylic adhesives property and optimized bonding parameters on Sn58Bi solder joint morphology for flex-on-board assembly. Microelectron. Reliab. **78**, 181–189 (2017)
4. M.Y. Xiong, L. Zhang, Interface reaction and intermetallic compound growth behavior of Sn-Ag-Cu lead-free solder joints on different substrates in electronic packaging. J. Mater. Sci. **54**, 1741–1768 (2019)
5. K.L. Lin, F.C. Chung, T.P. Liu, The potentiodynamic polarization behavior of Pb-free XIn-9(5Al-Zn)-YSn solders. Mater. Chem. Phys. **53**, 55–59 (1998)
6. L.C. Tsao, Corrosion characterization of Sn37Pb solders and with Cu substrate soldering reaction in 3.5wt.% NaCl solution. In: 2009 International Conference on Electronic Packaging Technology & High Density Packaging, 2009, pp. 1164–1166.
7. B. Liu, T.K. Lee, K.C. Liu, Impact of 5% NaCl salt spray pretreatment on the long-term reliability of wafer-level packages with Sn-Pb and Sn-Ag-Cu solder interconnects. J. Electron. Mater. **40**, 2111–2118 (2011)
8. L.M. Satizabal, D. Costa, P.B. Moraes et al., Microstructural array and solute content affecting electrochemical behavior of Sn Ag and Sn Bi alloys compared with a traditional Sn Pb alloy. Mater. Chem. Phys. **223**, 410–425 (2019)
9. M.A. Fazal, N.K. Liyana, S. Rubaiee et al., A critical review on performance, microstructure and corrosion resistance of Pb-free solders. Measurement **134**, 897–907 (2019)
10. H.A. Jaffery, M.F.M. Sabri, S.M. Said et al., Electrochemical corrosion behavior of Sn-0.7Cu solder alloy with the addition of bismuth and iron. J. Alloys Compd. **810**, 151925 (2019)
11. P. Tunthawiroon, K. Kanlayasiri, Effects of Ag contents in Sn-xAg lead-free solders on microstructure, corrosion behavior and interfacial reaction with Cu substrate. Trans. Nonferr. Met. Soc. **29**, 1696–1704 (2019)
12. F. Mohd Nazeri Muhammad, Z. Yahaya Muhamad, A. Gursel et al., Corrosion characterization of Sn-Zn solder: a review. Solder. Surf. Mater. Technol. **31**, 52–67 (2019)
13. Z. Hou, T. Niu, X. Zhao et al., Intermetallic compounds formation and joints properties of electroplated Sn-Zn solder bumps with Cu substrates. J. Mater. Sci. Mater. Electron. **30**, 1–9 (2019)
14. M.I.I. Ramli, M.A.A.M. Salleh, H. Yasuda, et al., The effect of Bi on the microstructure, electrical, wettability and mechanical properties of Sn-0.7Cu-0.05Ni alloys for high strength soldering. Mater. Design **186**, (2020).
15. M. Hasnine, M.J. Bozack, Effects of Ga additives on the thermal and wetting performance of Sn-0.7Cu solder. J. Electron. Mater. **48**, 3970–3978 (2019)
16. S. Tian, S. Li, J. Zhou et al., Thermodynamic characteristics, microstructure and mechanical properties of Sn-0.7Cu-xIn lead-free solder alloy. J. Alloys Compd. **742**, 835–843 (2018)
17. H. Ma, A. Kunwar, Z. Liu et al., Shielding effect of Ag_3Sn on growth of intermetallic compounds in isothermal heating and cooling during multiple reflows. J. Mater. Sci. Mater. Electron. **29**, 4383–4390 (2018)
18. L. Zhang, Z.Q. Liu, Inhibition of intermetallic compounds growth at Sn-58Bi/Cu interface bearing CuZnAl memory particles (2~6μm). J. Mater. Sci. Mater. Electron. **31**, 2466–2480 (2020)
19. Z. Wang, Q.K. Zhang, Y.X. Chen et al., Influences of Ag and In alloying on Sn-Bi eutectic solder and SnBi/Cu solder joints. J. Mater. Sci. Mater. Electron. **30**, 18524–18538 (2019)

20. N. Jiang, L. Zhang, Z.Q. Liu et al., Influences of doping Ti nanoparticles on microstructure and properties of Sn58Bi solder. J. Mater. Sci. Mater. Electron. **30**, 17583–17590 (2019)
21. J. Wu, S. Xue, J. Wang et al., Effect of in-situ formed Pr-coated Al_2O_3 nanoparticles on interfacial microstructure and shear behavior of Sn-03Ag-07Cu-006Pr/Cu solder joints during isothermal aging. J. Alloys Compd. **799**, 124–136 (2019)
22. Z. Zhang, X. Hu, X. Jiang, Y. Li, Influences of mono-Ni(P) and dual-Cu/Ni(P) plating on the interfacial microstructure evolution of solder joints. Metall. Mater. Trans. A **50**, 480–492 (2019)
23. W.K. Lee, X. Ning, C.B. Ke et al., Current density dependent shear performance and fracture behavior of micro-scale BGA structure Cu/Sn-3.0Ag-0.5Cu/Cu joints under coupled electromechanical loads. J. Mater. Sci. Mater. Electron. **30**, 15184–15197 (2019)
24. A.K. Gain, L. Zhang, Growth nature of in-situ Cu_6Sn_5-phase and their influence on creep and damping characteristics of Sn-Cu material under high-temperature and humidity. Microelectron. Reliab. **87**, 278–285 (2018)
25. T.K. Yeh, K.L. Lin, U.S. Mohanty, Effect of Ag on the microstructure of Sn-8.5Zn-xAg-0.01Al-0.1Ga solders under high-temperature and high-humidity conditions. J. Electron. Mater. **42**, 616–627 (2013)
26. M. Wang, J. Wang, H. Feng et al., Effect of Ag_3Sn intermetallic compounds on corrosion of Sn-3.0Ag-0.5Cu solder under high-temperature and high-humidity condition. Corros. Sci. **63**, 20–28 (2012)
27. K. Yokoyama, A. Nogami, J. Sakai, Creep corrosion cracking of Sn-3.0Ag and Sn-0.5Cu solder alloys in NaCl solution. Corros. Sci. **86**, 142–148 (2014)
28. Y.F. Gao, C.F. Cheng, J. Zhao et al., Electrochemical corrosion of Sn-0.75Cu solder joints in NaCl solution. Trans. Nonferr. Met. Soc. **22**, 977–982 (2012)
29. R.B. Comizzoli, R.P. Frankenthal, P.C. Milner et al., Corrosion of electronic materials and devices. Science **234**, 340–345 (1986)
30. J.C. Liu, Z.H. Wang, J.Y. Xie et al., Understanding corrosion mechanism of Sn-Zn alloys in NaCl solution via corrosion products characterization. Mater. Corros. **67**, 522–530 (2016)
31. J.C. Liu, Z.H. Wang, J.Y. Xie et al., Effects of intermetallic-forming element additions on microstructure and corrosion behavior of Sn-Zn solder alloys. Corros. Sci. **112**, 150–159 (2016)
32. M. Wang, J. Wang, H. Feng et al., Effects of microstructure and temperature on corrosion behavior of Sn-3.0Ag-0.5Cu lead-free solder. J. Mater. Sci. Mater. Electron. **23**, 148–155 (2011)
33. Z. Yan, A.P. Xian, Pitting corrosion behavior of Sn-0.7Cu lead-free alloy in simulated marine atmospheric enviroment and the effect of trace Ga. Acta Metal. Sin. **47**, 1327–1334 (2011)
34. Z. Yan, A.P. Xian, Initial corrosion behavior of Sn and Sn-3Ag-0.5Cu alloy exposed in atmospheric environment of Shenyang. Chin. J. Nonfer. Met. **22**, 1398–1406 (2012)
35. B. Liao, H. Cen, Z. Chen et al., Corrosion behavior of Sn-3.0Ag-0.5Cu alloy under chlorine-containing thin electrolyte layers. Corros. Sci. **143**, 347–361 (2018)
36. X.K. Zhong, G.A. Zhang, Y.B. Qiu et al., The corrosion of tin under thin electrolyte layers containing chloride. Corros. Sci. **66**, 14–25 (2013)
37. Z. Wang, C. Chen, J. Liu et al., Corrosion mechanism of Zn-30Sn high-temperature, lead-free solder in neutral NaCl solution. Corros. Sci. **140**, 40–50 (2018)
38. J.C. Liu, G. Zhang, Effect of trace Mn modification on the microstructure and corrosion behavior of Sn-9Zn solder alloy. Mater. Corros. **69**, 781–792 (2018)
39. Z. Wang, C. Chen, J. Jiu et al., Electrochemical behavior of Sn-9Zn-xTi lead-free solders in neutral 0.5M NaCl solution. J. Mater. Eng. Perform. **27**, 2182–2191 (2018)
40. Z. Wang, C. Chen, J. Jiu et al., Electrochemical behavior of Zn-x Sn high-temperature solder alloys in 0.5 M NaCl solution. J. Alloys Compd. **716**, 231–239 (2017)
41. D. Li, P.P. Conway, C. Liu, Corrosion characterization of tin-lead and lead free solders in 3.5 wt% NaCl solution. Corros. Sci. **50**, 995–1004 (2008)
42. H. Huang, G. Shuai, X. Wei et al., Effects of sulfur addition on the wettability and corrosion resistance of Sn-0.7Cu lead-free solder. Microelectron. Reliab. **74**, 15–21 (2017)
43. H. Wang, Z. Gao, Y. Liu et al., Evaluation of cooling rate on electrochemical behavior of Sn-0.3Ag-0.9Zn solder alloy in 3.5wt% NaCl solution. J. Mater. Sci. Mater. Electron. **26**, 11–22 (2014)
44. N.W.B. Subri, M. Sarraf, B. Nasiri-Tabrizi et al., Corrosion insight of iron and bismuth added Sn-1Ag-0.5Cu lead-free solder alloy. Corros. Eng. Sci. Techn. **55**, 35–47 (2020)
45. N.K. Liyana, M.A. Fazal, A.S.M.A. Haseeb et al., Effect of Zn incorporation on the electrochemical corrosion properties of SAC105 solder alloys. J. Mater. Sci. Mater. Electron. **30**, 7415–7422 (2019)
46. M. Fayeka, M.A. Fazal, A.S.M.A. Haseeb, Effect of aluminum addition on the electrochemical corrosion behavior of Sn-3Ag-0.5Cu solder alloy in 3.5wt% NaCl solution. J. Mater. Sci. Mater. Electron. **27**, 12193–12200 (2016)
47. M. Liu, W. Yang, Y. Ma et al., The electrochemical corrosion behavior of Pb-free Sn-8.5Zn-XCr solders in 3.5 wt.% NaCl solution. Mater. Chem. Phys. **168**, 27–34 (2015)
48. M. Wang, J. Wang, W. Ke, Corrosion behavior of Sn-3.0Ag-0.5Cu solder under high-temperature and high-humidity condition. J. Mater. Sci. Mater. Electron. **25**, 1228–1236 (2014)
49. M. Wang, J. Wang, W. Ke, Effect of microstructure and Ag_3Sn intermetallic compounds on corrosion behavior of Sn-3.0Ag-0.5Cu lead-free solder. J. Mater. Sci. Mater. Electron. **25**, 5269–5276 (2014)
50. X. Zhong, G. Zhang, X. Guo, The effect of electrolyte layer thickness on electrochemical migration of tin. Corros. Sci. **96**, 1–5 (2015)
51. X. Zhong, G. Zhang, Y. Qiu et al., Electrochemical migration of tin in thin electrolyte layer containing chloride ions. Corros. Sci. **74**, 71–82 (2013)
52. T.C. Chang, M.H. Hon, M.C. Wang et al., Electrochemical behaviors of the Sn-9Zn-xag lead-free solders in a 3.5 wt % NaCl solution. J. Electrochem. Soc. **151**, C484 (2004)
53. M.F.M. Nazeri, A.A. Mohamad, Effect of exposure to alkaline solution on Sn-9Zn solder joints. J. Mater. Process. Technol. **219**, 164–172 (2015)
54. M. Grobelny, N. Sobczak, Effect of pH of sulfate solution on electrochemical behavior of Pb-Free solder candidates of SnZn and SnZnCu systems. J. Mater. Eng. Perform. **21**, 614–619 (2012)
55. S. Farina, C. Morando, Comparative corrosion behaviour of different Sn-based solder alloys. J. Mater. Sci. Mater. Electron. **26**, 464–471 (2014)
56. J.C. Liu, S. Park, S. Nagao et al., The role of Zn precipitates and Cl^- anions in pitting corrosion of Sn-Zn solder alloys. Corros. Sci. **92**, 263–271 (2015)
57. J.C. Liu, G. Zhang, S. Nagao et al., Metastable pitting and its correlation with electronic properties of passive films on Sn-xZn solder alloys. Corros. Sci. **99**, 154–163 (2015)
58. J.C. Liu, G. Zhang, J.S. Ma et al., Ti addition to enhance corrosion resistance of Sn-Zn solder alloy by tailoring microstructure. J. Alloys Compd. **644**, 113–118 (2015)
59. M.F. Mohd Nazeri, A.A. Mohamad, Corrosion resistance of ternary Sn-9Zn-xIn solder joint in alkaline solution. J. Alloys Compd. **661**, 516–525 (2016)
60. H. Wang, S.B. Xue, W.X. Chen et al., Effects of Ga and Al additions on corrosion resistance and high-temperature oxidation

resistance of Sn-9Zn lead-free solder. Rare Metal. Mat. Eng. **38**, 2187–2190 (2009)
61. M.F.M. Nazeri, A.A. Mohamad, Corrosion measurement of Sn-Zn lead-free solders in 6 M KOH solution. Measurement **47**, 820–826 (2014)
62. M.F.M. Nazeri, A.B. Ismail, A.A. Mohamad, Effect of polarizations on Sn-Zn solders alloys in alkaline electrolyte. J. Alloys Compd. **606**, 278–287 (2014)
63. X.K. Zhong, L.J. Chen, B. Medgyes et al., Electrochemical migration of Sn and Sn solder alloys: a review. RSC Adv. **7**, 28186–28206 (2017)
64. Q. Li, X. Liu, S. Lu, Corrosion behavior assessment of tin-lead and lead free solders exposed to fire smoke generated by burning polyvinyl chloride. Mater. Chem. Phys. **212**, 298–307 (2018)
65. W.R. Osório, J.E. Spinelli, C.R.M. Afonso et al., Microstructure, corrosion behaviour and microhardness of a directionally solidified Sn-Cu solder alloy. Electrochim. Acta **56**, 8891–8899 (2011)
66. W.R. Osório, E.S. Freitas, J.E. Spinelli et al., Electrochemical behavior of a lead-free Sn-Cu solder alloy in NaCl solution. Corros. Sci. **80**, 71–81 (2014)
67. E.S. Freitas, W.R. Osório, J.E. Spinelli et al., Mechanical and corrosion resistances of a Sn-0.7wt%Cu lead-free solder alloy. Microelectron. Reliab. **54**, 1392–1400 (2014)
68. W. Yang, Z. Du, S. Yu et al., The effect of rare earths additions on the microstructure and the corrosion behavior of Sn-0.7Cu-0.075Al solder alloy. Materials **12**, 3731 (2019)
69. H.Z. Huang, D. Lu, G.W. Shuai et al., Effects of phosphorus addition on the corrosion resistance of Sn-0.7Cu lead-free solder alloy. T. Indian. I. Metals **69**, 1537–1543 (2016)
70. Z. Yan, A.P. Xian, Corrosion of Ga-doped Sn-0.7Cu solder in simulated marine atmosphere. Metall. Mater. Trans. A **44**, 1462–1474 (2012)
71. A.K. Gain, L. Zhang, Thermal aging effects on microstructure, elastic property and damping characteristic of a eutectic Sn-3.5Ag solder. J. Mater. Sci. Mater. Electron. **29**, 14519–14527 (2018)
72. S. Liu, W. Xiong, J. Xiong et al., Refinement mechanism of Bi addition on the microstructure of rapidly solidified Sn-3.5Ag eutectic solder for microelectronic packaging. J. Electron. Mater. **47**, 5588–5594 (2018)
73. J. Li, J. Dai, C.M. Johnson, Comparison of power cycling reliability of flexible PCB interconnect smaller/thinner and larger/thicker power devices with topside Sn-3.5Ag solder joints. Microelectron. Reliab. **84**, 55–65 (2018)
74. Q.V. Bui, N.D. Nam, B.I. Noh et al., Effect of Ag addition on the corrosion properties of Sn-based solder alloys. Mater. Corros. **61**, 30–33 (2010)
75. M.A. Ameer, A.A. Ghoneim, A.M. Fekry, The electrochemical behavior of Sn-Ag binary alloys in sulfate solutions. Mater. Corros. **61**, 580–589 (2010)
76. M.A. Ameer, A.M. Fekry, A.A. Ghoniem, Electrochemical behavior of Sn-Ag alloys in alkaline solutions. Corrosion **65**, 587–594 (2009)
77. F. Ochoa, J.J. Williams, N. Chawla, Effects of cooling rate on the microstructure and tensile behavior of a Sn-3.5wt.%Ag solder. J. Electron. Mater. **32**, 1414–1420 (2003)
78. J. Shen, Y.C. Liu, Y.J. Han et al., Effects of cooling rates on microstructure and microhardness of lead-free Sn-3.5% Ag solders. Trans. Nonferr. Met. Soc. **16**, 59–64 (2006)
79. L.R. Garcia, W.R. Osório, A. Garcia, The effect of cooling rate on the dendritic spacing and morphology of Ag_3Sn intermetallic particles of a SnAg solder alloy. Mater. Design **32**, 3008–3012 (2011)
80. X. Liu, M. Huang, Y. Zhao et al., The adsorption of Ag_3Sn nanoparticles on Cu-Sn intermetallic compounds of Sn-3Ag-0.5Cu/Cu during soldering. J. Alloys Compd. **492**, 433–438 (2010)
81. W.R. Osório, L.R. Garcia, L.C. Peixoto et al., Electrochemical behavior of a lead-free SnAg solder alloy affected by the microstructure array. Mater. Design **32**, 4763–4772 (2011)
82. B.X. Vuong, N.S.H. Vu, T.D. Manh et al., Role of cerium in microstructure and corrosion properties of Sn-1.0Ag solder alloys. Mater. Lett. **228**, 309–313 (2018)
83. A. Sharma, S. Das, K. Das, Electrochemical corrosion behavior of CeO_2 nanoparticle reinforced Sn-Ag based lead free nanocomposite solders in 3.5 wt% NaCl bath. Surf. Coat. Technol. **261**, 235–243 (2015)
84. F. Rosalbino, E. Angelini, G. Zanicchi et al., Corrosion behaviour assessment of lead-free Sn-Ag-M (M=In, Bi, Cu) solder alloys. Mater. Chem. Phys. **109**, 386–391 (2008)
85. X. Li, Y. Ma, W. Zhou et al., Effects of nanoscale Cu_6Sn_5 particles addition on microstructure and properties of SnBi solder alloys. Mater. Sci. Eng. A **684**, 328–334 (2017)
86. M. Mostofizadeh, J. Pippola, L. Frisk, Reliability and shear strength of 42Sn-57Bi-1Ag (wt.%) lead-free solder joints after thermal aging and salt spray testing. In: 2013 IEEE 63rd Electronic Components and Technology Conference, 2013, pp. 1010–1017.
87. L.M. Satizabal, E. Poloni, A.D. Bortolozo et al., Immersion corrosion of Sn-Ag and Sn-Bi alloys as successors to Sn-Pb alloy with electronic and jewelry applications. Corrosion **72**, 1064–1080 (2016)
88. M. Mostofizadeh, J. Pippola, T. Marttila et al., Effect of thermal aging and salt spray testing on reliability and mechanical strength of Sn-58Bi lead-free solder. IEEE T. Comp. Pack. Man. **3**, 1778–1785 (2013)
89. X. Qiang, L. Nguyen, W.D. Armstrong, Anomalously high tensile creep rates from thin cast Sn3.9Ag0.6Cu lead-free solder. J. Electron. Mater. **34**, 1065-1075.
90. J.P. Tucker, D.K. Chan, G. Subbarayan et al., Maximum entropy fracture model and its use for predicting cyclic hysteresis in Sn3.8Ag0.7Cu and Sn3.0Ag0.5 solder alloys. Microelectron. Reliab. **54**, 2513–2522 (2014)
91. D. Chan, X. Nie, D. Bhate et al., Constitutive models for intermediate-and high-strain rate flow behavior of Sn3.8Ag0.7Cu and Sn1.0Ag0.5Cu solder alloys. IEEE T. Comp. Pack. Man. **3**, 133–146 (2013)
92. M.N. Wang, J.Q. Wang, W. Ke, Corrosion behavior of Sn-3.0Ag-0.5Cu lead-free solder joints. Microelectron. Reliab. **73**, 69–75 (2017)
93. C.W. See, M.Z. Yahaya, H. Haliman et al., Corrosion behavior of corroded Sn-3.0Ag-0.5Cu solder alloy. Procedia Chem **19**, 847–854 (2016)
94. F. Rosalbino, G. Zanicchi, R. Carlini et al., Electrochemical corrosion behaviour of Sn-Ag-Cu (SAC) eutectic alloy in a chloride containing environment. Mater. Corros. **63**, 492–496 (2012)
95. F. Rosalbino, E. Angelini, G. Zanicchi et al., Electrochemical corrosion study of Sn-3Ag-3Cu solder alloy in NaCl solution. Electrochim. Acta **54**, 7231–7235 (2009)
96. L. Hua, C. Yang, Corrosion behavior, whisker growth, and electrochemical migration of Sn-3.0Ag-0.5Cu solder doping with In and Zn in NaCl solution. Microelectron. Reliab. **51**, 2274–2283 (2011)
97. N.I.M. Nordin, S.M. Said, R. Ramli et al., Impact of aluminium addition on the corrosion behaviour of Sn-1.0Ag-0.5Cu lead-free solder. Rsc Adv **5**, 99058–99064 (2015)
98. U.S. Mohanty, K.-L. Lin, Corrosion behavior of Pb-free Sn-1Ag-0.5Cu-XNi Solder Alloys in 3.5% NaCl Solution. J. Electron. Mater. **42**, 628–638 (2013)
99. L.Y. Xu, Z.K. Zhang, H.Y. Jing et al., Effect of graphene nanosheets on the corrosion behavior of Sn-Ag-Cu solders. J. Mater. Sci. Mater. Electron. **26**, 5625–5634 (2015)

100. Y.D. Han, L. Chen, H.Y. Jing et al., Effect of Ni-Coated carbon nanotubes on the corrosion behavior of Sn-Ag-Cu solder. J. Electron. Mater. **42**, 3559–3566 (2013)
101. W. Jie, X. Songbai, W. Jingwen et al., Enhancement on the high-temperature joint reliability and corrosion resistance of Sn-0.3Ag-0.7Cu low-Ag solder contributed by Al_2O_3 Nanoparticles (0.12 wt%). J. Mater. Sci. Mater. Electron. **29**, 19663–19677 (2018)
102. A.A. El-Daly, K.M. Zohdy, M. Ragab, Corrosion and electrochemical behavior of Sn-2Ag-0.5Cu lead-free solders solidified with magnet stirring. J. Mater. Eng. Perform. **28**, 4680–4692 (2019)
103. T.K. Lee, B. Liu, B. Zhou et al., Correlation between sn grain orientation and corrosion in Sn-Ag-Cu solder interconnects. J. Electron. Mater. **40**, 1895–1902 (2011)
104. M. Wang, J. Wang, H. Feng et al., In-situ observation of fracture behavior of Sn-3.0Ag-0.5Cu lead-free solder during three-point bending tests in ESEM. Mater. Sci. Eng. A **558**, 649–655 (2012)
105. R.K. Kaushik, U. Batra, J.D. Sharma, Aging induced structural and electrochemical corrosion behaviour of Sn-1.0Ag-0.5Cu and Sn-3.8Ag-0.7Cu solder alloys. J. Alloys Compd. **745**, 446–454 (2018)
106. U.S. Mohanty, K.-L. Lin, Electrochemical corrosion behaviour of lead-free Sn-8.5 Zn-X Ag-0.1 Al-0.5 Ga solder in 3.5% NaCl solution. Mater. Sci. Eng.: A **406**, 34-42 (2005).
107. U.S. Mohanty, K.-L. Lin, The polarization characteristics of Pb-free Sn-8.5Zn-XAg-0.1Al-0.05Ga alloy in 3.5% NaCl solution. Corros. Sci. **49**, 2815-2831 (2007).
108. U.S. Mohanty, K.-L. Lin, Effect of Al on the electrochemical corrosion behaviour of Pb free Sn-8.5 Zn-0.5 Ag-XAl-0.5 Ga solder in 3.5% NaCl solution. Appl. Surf. Sci. **252**, 5907-5916 (2006).
109. U.S. Mohanty, K.-L. Lin, The effect of alloying element gallium on the polarization characteristics of Pb-free Sn-Zn-Ag-Al-XGa solders in NaCl solution. Corros. Sci. **48**, 662–678 (2006)
110. T.C. Chang, J.W. Wang, M.C. Wang et al., Solderability of Sn-9Zn-0.5Ag-1In lead-free solder on Cu substrate. J. Alloys Compd. **422**, 239–243 (2006)
111. J. Hu, T. Luo, A. Hu et al., Electrochemical corrosion behaviors of Sn-9Zn-3Bi-xCr solder in 3.5% NaCl solution. J. Electron. Mater. **40**, 1556–1562 (2011)
112. K.L. Lin, T.P. Liu, The electrochemical corrosion behaviour of Pb-free Al-Zn-Sn solders in NaCl solution. Mater. Chem. Phys. **56**, 171–176 (1998)
113. M.L. Huang, N. Kang, Q. Zhou et al., Effect of Ni content on mechanical properties and corrosion behavior of Al/Sn-9Zn-xNi/Cu joints. J. Mater. SCI. Technol. **28**, 844–852 (2012)